Boundary-Layer Meteorol (2007) 122:17–29
DOI 10.1007/s10546-006-9090-4

ORIGINAL PAPER

Sea-breeze scaling from numerical model simulations, Part I: Pure sea breezes

Aurore Porson · Douw G. Steyn · Guy Schayes

Received: 24 September 2005 / Accepted: 14 April 2006 /
Published online: 21 October 2006

Abstract Numerical model simulations of sea-breeze circulations under idealized conditions are subjected to dimensional analyses in order to resolve sea-breeze dynamical relations and unify previous results based on observations. The analysis is motivated by the fact that sea-breeze depth scaling and volume flux scaling are only partially understood. The analysis is based on nonlinear numerical modelling simulations in combination with recent observational scaling analyses. The analysis confirms scaling laws for sea-breeze strength dependence on governing variables and shows how the sea-breeze speed scale is controlled by surface heat flux. It also shows that the sea-breeze depth scale is controlled by stability. By combining sea-breeze speed and depth scales, the sea-breeze volume flux scale is determined by an equilibrium between the accumulated convergence of heat over land since sunrise and stable air advection from the sea surface.

Keywords Numerical model · Scaling law · Sea breeze · Surface heat flux · Stability · Volume flux scaling

1 Introduction

Sea breezes are mesoscale circulations driven by differential heating between sea and land. These circulations usually appear in the form of a landward inflow layer

A. Porson · G. Schayes
Institut d'Astronomie et de Géophysique Georges Lemaître,
Université Catholique de Louvain, Brussels, Belgium

D. G. Steyn
Department of Earth and Ocean Sciences, University of British Columbia,
Vancouver, BC, Canada

A. Porson (✉)
Department of Meteorology, University of Reading,
RG6 6BB, PO Box 243, Reading, UK
e-mail: a.m.f.porson@reading.ac.uk

of defined speed and depth, surmounted by a return flow of equivalent mass flux. Sea-breeze circulations have a strong influence on coastal zone meteorology and are important in the fields of weather forecasting, climatology and air pollution dispersion. The effects of sea breezes on human beings may be significant: reduced air quality and related health problems, thunderstorm development and agricultural productivity. Sea breezes are also interesting for their use in offshore wind energy production, and so it is important to continue improving our understanding of sea-breeze dynamics and their interaction with the environment.

Sea-breeze speed dependence on governing variables has recently been studied using scaling techniques by Tijm et al. (1999a), Steyn (2003) and Wichink Kruit et al. (2004). Defining the sea-breeze speed U_{sb} as:

$$U_{\mathrm{sb}} = \frac{1}{Z_{\mathrm{sb}}} \int_0^{Z_{\mathrm{sb}}} U \, \mathrm{d}Z, \tag{1}$$

in which Z_{sb} is the sea-breeze depth (the height at which the horizontal wind component U first reaches zero), Steyn (2003) found the following sea-breeze speed scaling from observational data for Vancouver (Canada), Burriana (Spain) and the Netherlands:

$$\frac{U_{\mathrm{sb}}}{u_{\mathrm{s}}} = 0.85\, \Pi_1^{-1/2} \Pi_4^{1/2} \Pi_2^{-9/4}, \tag{2}$$

with the velocity scale $u_{\mathrm{s}} = g \triangle T/TN$, the non-dimensional groups Π_1, Π_4, Π_2 as defined in Table 1 and the governing parameters ω = the Earth's diurnal rotation frequency, $\triangle T$ = the land-sea temperature difference, T = the reference temperature of the boundary layer, N = the Brunt–Väisälä frequency, f = the Coriolis parameter, H = the time-averaged integrated (kinematic) surface heat flux = $\frac{1}{t_{\mathrm{p}}} \int_0^{t_{\mathrm{p}}} \overline{(w'\theta')_{\mathrm{s}}} \, \mathrm{d}t$ with t_{p} the time integration period since sunrise, and g/T = the buoyancy parameter. At a latitude of 50° (the latitude of Vancouver), the sea-breeze speed dependence on governing variables from Eq. 2 is given by

$$U_{\mathrm{sb}} = 0.33 \left(\frac{gH}{T\omega} \right)^{1/2}. \tag{3}$$

From Eq. 3, the sea-breeze speed is independent of stability, while the time-averaged integrated surface heat flux H measured near the coastline captures the mechanism of surface heating better than the land-sea temperature difference $\triangle T$. This behaviour was corroborated by an independent set of data over the Netherlands by Wichink Kruit et al. (2004), whose study was based on surface heat flux estimates made inland (rather than near the coastline).

Table 1 Non-dimensional groups

Π_1	=	$\frac{g\Delta T^2}{NTH}$	Π_2	=	$\frac{f}{\omega}$
			Π_4	=	$\frac{N}{\omega}$
u_{s}	=	$\frac{g\Delta T}{TN}$	z_{s}	=	$\frac{H}{\omega \Delta T}$

The coastal zone surface heat flux cannot be seen as an external parameter to the sea-breeze circulation, in contrast to the land-sea temperature difference for which the land temperature is measured far away from the coastline, or to the surface heat flux measured away from the coastline. We argue that the coastal zone surface heat flux is more appropriate, with two arguments to justify the use of the coastal zone surface heat flux rather than the surface heat flux measured away from coastline. First, Arritt (1987) emphasized the role of the surface heat flux measured near the coastline in order to capture the state of stability over the sea surface. Second, when comparing the studies of Steyn (2003) with that of Wichink Kruit et al. (2004), the surface heat flux measured in the coastal zone and the surface heat flux measured away from the coastal zone can be related to each other. Indeed, as mentioned earlier, Wichink Kruit et al. reproduced the scaling laws developed by Steyn, while measurements of surface heat flux in the first study were obtained away from the coastline and measurements in the second study were obtained in the coastal zone. Wichink Kruit et al. showed that the difference between the two studies has a proportionality factor of the order of two. This factor can be justified by stronger values of coastal surface heat flux relative to inland values of surface heat flux. From numerical simulations, it was verified that the ratio of the two types of measurement of surface heat flux is constant and independent of stability variations.

The use of the coastal surface heat flux is also more appropriate than the land-sea temperature difference because of the following reasons. From the observations over Vancouver in July and August 1983, 1985 and 1986, the time-averaged integrated surface heat flux can be related to the land-sea temperature difference over a diurnal period as suggested in Fig. 1. However, when one analyses Fig. 1 at a specific time, the relationship between the two variables is ill-defined and it is possible to further argue in respect of the surface heat flux. Indeed, according to Pielke and Segal (1986), the time-averaged integrated surface heat flux is a more appropriate variable than the land-sea temperature difference because it includes the vertical integration of the land-sea temperature difference.

Tijm et al. (1999a) obtained a relation very close to Eq. 3 but with a weak inverse dependence $(-1/4)$ on N. These studies of sea-breeze speed are also similar to the study of gravity currents developed by Simpson (1969) who obtained a speed dependence on $\sqrt{\triangle T}$.

There are however fewer studies of sea-breeze depth dependence on governing variables and these studies show very large scatter (Walsh 1974; Tijm et al. 1999a; Steyn 2003). Walsh (1974) obtained a sea-breeze depth scale dependent on eddy coefficients of viscosity and of heat while Steyn (1998) explained that the use of eddy coefficients is not appropriate for sea-breeze scaling. Tijm et al. (1999b) found that the boundary-layer height is a relevant length scale for sea-breeze depth. Given a length scale $z_s = H/\omega \triangle T$, Steyn (2003) showed that the sea-breeze depth Z_{sb} can be scaled as:

$$\frac{Z_{sb}}{z_s} = 0.75\, \Pi_1^{1/3} \Pi_2^{-5/2}, \tag{4}$$

which gives, at the latitude of 50°,

$$Z_{sb} = \frac{0.26}{\omega} \left(\frac{gH^2}{NT \triangle T} \right)^{1/3}. \tag{5}$$

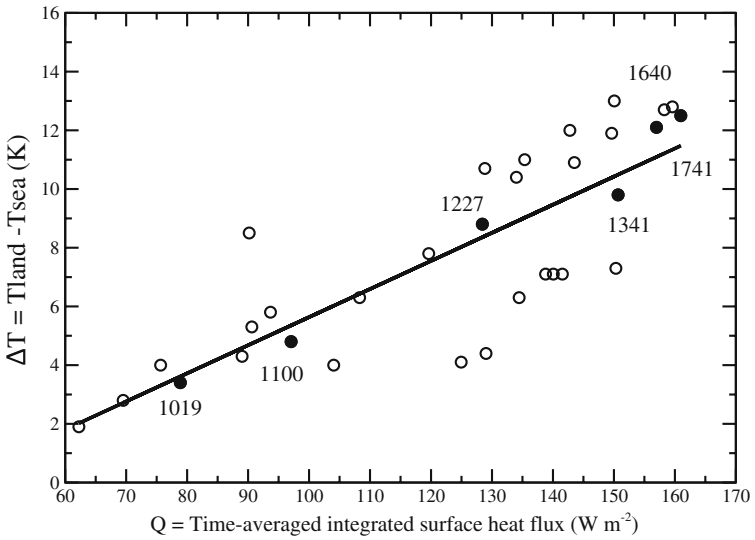

Fig. 1 Observations from Steyn (1998). Data are taken during the months of July and August for 1983, 1985 and 1986. The difference between near-surface air temperature over land, approximately 50 km from the coast, and sea surface temperature is shown as a function of the integrated surface heat flux since sunrise. Hours in local time are indicated to retrace the time evolution for data from 23 August 1985. A linear regression, depicted by the black line, gives: $\Delta T = -3.94 + 0.096\,Q$, with a correlation coefficient of 0.81 and standard errors of estimate of 1.55 for the intercept and 0.012 for the coefficient

To understand sea-breeze dynamics further, sea-breeze depth scaling will be revisited. Considering that the product of sea-breeze depth and sea-breeze speed yields the volume flux, understanding sea-breeze depth dependence on governing variables implies also understanding the sea-breeze volume flux dependence.

We use here the nonlinear numerical mesoscale model TVM to provide a scaling analysis from idealized 2D simulations. Although Steyn's scaling collapses at the equator ($f = 0$), we will not investigate here the dependence on latitude and we will work at a fixed latitude of 50° N. The research questions and objectives that will be addressed are:

- Can the numerical model reproduce sea-breeze speed scaling dependence as captured by recent studies based on observations? More generally, can the flexibility of a numerical model be used to conduct a more extensive scaling analysis than is possible with observations?
- Can we use the conclusions of earlier work that sea-breeze scaling is independent of land-sea temperature difference to revisit the dependence of sea-breeze depth? Is this independence supported by other published results?
- What are the scaling laws for the sea-breeze volume flux?

2 Model description

TVM is a meso-γ scale atmospheric model fully described in Schayes et al. (1996) and in Thunis and Clappier (2000). Prognostic variables are potential temperature,

turbulent kinetic energy and two horizontal vorticity components. The calculation of vorticity components avoids integration of the dynamical pressure and air density. In this model, the surface temperature evolves using the force-restore soil model of Deardoff (1978). A (dry) non-saturated atmosphere is assumed; infra-red absorption by water vapour is neglected in the model; a constant geostrophic wind forcing is applied through the atmosphere; the non-hydrostatic and anelastic version is used. A numerical diffusion filter for high spatial wavenumbers was employed to avoid perturbations triggered by convection (Raymond and Garder 1988), and this proved to be more efficient than a higher and constant horizontal diffusion coefficient (Arritt 1989). The model employs a 1.5-order turbulence scheme, and uses the mixing length formulation of Bougeault and Lacarrère (1989). TVM will be operated in 2D in a vertical plane along the west–east direction. Parameters are listed in Table 2.

The simulations are conducted by varying the initial conditions for the potential temperature vertical gradient γ over a range of 10 values, as $\gamma_i\,(\text{in K km}^{-1}) = 1.65+0.5i$ with $i = 0, 9$. There are 60 vertical levels covering more than 7000 m, and a fine grid increment of 50 m is used from 200 m up to 1300 m; below 200 m, the resolution is progressively increased from 15 to 50 m and above 1300 m, the resolution decreases progressively to reach finally 400 m at the uppermost levels. Figure 2 illustrates how the model captures a sea-breeze circulation in wind component and potential temperature at 1500 LST. The sea-breeze speed and depth were averaged over the second and third inland grid points (at 6 km from the coastline), and the time-integrated surface heat flux is calculated over the first three inland grid points. In the afternoon, this variable remains roughly constant with its maximum at 1500 LST.

3 Scaling sea-breeze speed

We examine now whether or not TVM is capable of capturing the scaling of sea-breeze speed as in Eq. 2.

Sea-breeze intensity at 1400 LST, 1500 LST and 1600 LST are extracted from model output, and a multiple regression performed between the dimensionless groups Π_1 and Π_4 on the scaled sea-breeze speed $U_{\text{sb}}/u_{\text{s}}$, yielding:

Table 2 TVM parameters

Horizontal resolution	3 km
General time step	25 s
Sea length or land length	200 km
Latitude	50° N
Time of the year	30 June
Geostrophic wind speed	$0\,\text{m s}^{-1}$
Sea surface temperature (SST) = Initial soil temperature	293 K
Land emissivity	0.95
Land surface roughness	0.1 m
Surface resistance to evaporation	$300\,\text{s m}^{-1}$
Land Albedo	0.2
Soil heat capacity	$1.5 \times 10^5\,\text{J m}^{-3}\text{K}^{-1}$
Run duration	19 h

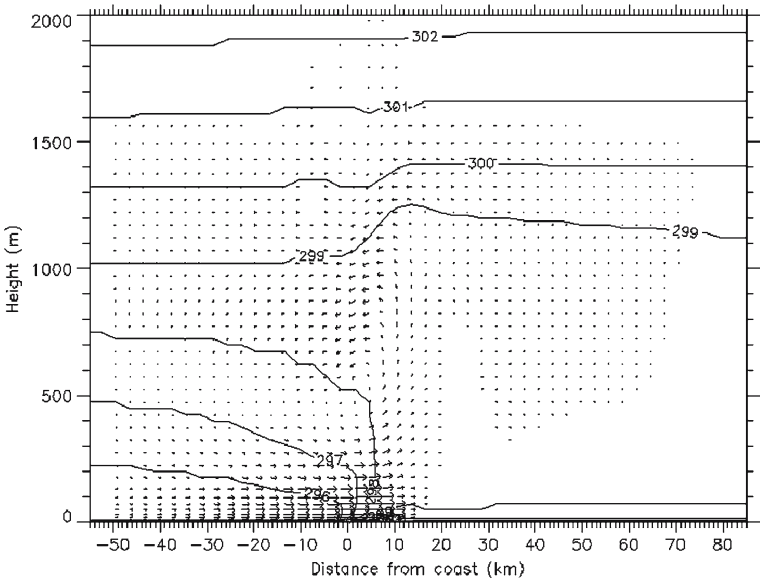

Fig. 2 Representation of the sea-breeze circulation in a vertical plane along the west–east direction. The wind component is depicted with wind vectors for which the vertical velocity has been increased by a factor of 300. The contours of potential temperature are represented by solid lines

$$\frac{U_{\mathrm{sb}}}{u_{\mathrm{s}}} = 0.687\,\Pi_1^{-1/2}\Pi_4^{1/3}, \tag{6}$$

with a standard deviation of 0.009 on the coefficient (Fig. 3). Wichink Kruit et al. (2004) showed that the scaling analysis developed by Steyn (2003) includes hidden correlation analysis. However, Wichink Kruit et al. (2004) showed that for some cases, the statistical analysis can be robust; for example, when the sea-breeze circulation reaches its maximum intensity and when the surface heat flux variable is integrated over time. These two cases are considered here, and to demonstrate that hidden correlation does not influence the present results, we will show later a plot of the non-scaled volume flux. As shown in Fig. 3, the model reproduces well the scaling analysis from observations. Indeed, Eq. 6 differs from Eq. 2 by a weaker dependence on Π_4 (1/3 instead of 1/2), which yields, in comparison to Eq. 3, an additional dependence on N of approximately -0.17. This difference lies in the range of the numerical study of Tijm et al. (1999a) who found an additional dependence of $-1/4$.

Therefore, considering that the additional dependence on N is minor compared to the dependence on surface heating H, we conclude that TVM reproduces the sea-breeze speed scaling of recent observational studies. If we neglect the slight difference in stability dependence from Steyn's scaling law in Eq. 3 between the studies of Tijm et al. (1999a), Steyn (2003) and Wichink Kruit et al. (2004) and the present one, we can use the velocity scale u_{sscale}:

$$u_{\mathrm{sscale}} = \left(\frac{gH}{T\omega}\right)^{1/2}.$$

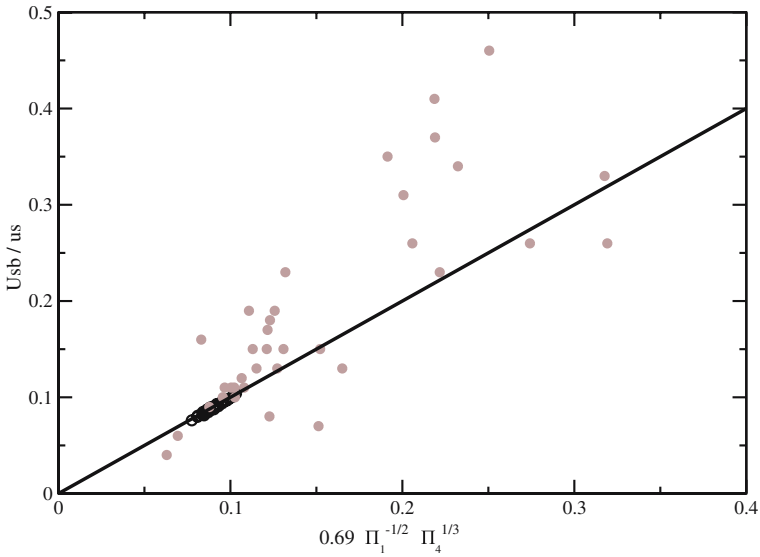

Fig. 3 Model data for $[U_{sb}/u_s]$ as a function of the regression in Eq. 6. The full black line is the one to one relationship. Ten groups of stability γ_i are represented for 1400 LST, 1500 LST and 1600 LST (black symbols). Observations from Vancouver (Steyn 2003) are also plotted in grey and filled circles

4 Scaling sea-breeze volume flux

4.1 Development of a volume flux scale

The volume flux scale is based on scales for sea-breeze depth and speed. The depth scale will be derived from two different approaches, both leading to identical results, thus strengthening our confidence in the correctness of the overall flux scaling.

The first approach is based on Tijm et al. (1999b) who showed that the initial boundary-layer depth is a suitable scale for the sea-breeze depth. However, the use of the boundary-layer height remains impractical for measurements since the boundary-layer height is controlled by governing parameters. We aim therefore at developing a sea-breeze depth scale based on the similarity with the boundary-layer height scale. Because sea breezes become established after the initiation of convection inland, the scale of the boundary-layer depth in idealized convective conditions (Stull 1988) can be used to develop a sea-breeze vertical length scale z_{sscale}. Stull (1988) obtained the following convective boundary-layer formulation in the absence of advection and subsidence effects:

$$z_i^2 - z_{i0}^2 = \frac{2}{\gamma}\left[\overline{w'\theta'_s} - \overline{w'\theta'_{z_i}}\right](t - t_0), \tag{7}$$

where $t - t_0$ represents the integration period of the surface heat flux $\overline{w'\theta'_s}$ and z_i the convective boundary-layer height. If one assumes that surface heating is the only source of warming in the boundary layer, then the heat flux at z_i becomes 0. If, in addition, the time integration period is taken to start at sunrise, $z_{i0} = 0$ and $t - t_0 = t_p$.

As N is equal to $\sqrt{g\gamma/T}$ and as $1/T$ is roughly constant, Eq. 7 yields:

$$z_i^2 = 2\frac{g}{TN^2}\,\overline{(w\theta')_s}\,t_p. \tag{8}$$

As the surface heat flux varies from sunrise, Eq. 8 can be used to determine z_{sscale} by the use of the time-averaged surface heat flux H and the frequency ω:

$$z_{sscale} = \left(\frac{gH}{T\omega}\right)^{1/2}\frac{1}{N}. \tag{9}$$

The second approach is based on the analysis of sea-breeze depth from TVM model output. A multiple regression with Π_1 and Π_4 yields:

$$\frac{Z_{sb}}{z_s} = 0.331\,\Pi_1^{1/2}\Pi_4^{-1/3}, \tag{10}$$

with a standard error of estimate on the coefficient of 0.007 (Fig. 4). Eq. 10 leads to:

$$Z_{sb} = 0.331\varepsilon\left(\frac{gH}{T\omega}\right)^{1/2}\frac{1}{N}, \tag{11a}$$

$$0.331\varepsilon = \left(\frac{N}{\omega}\right)^{1/6} \approx \text{constant}, \tag{11b}$$

which is in agreement with the definition of z_{sscale} in Eq. 9. As illustrated in Fig. 4, this form is somewhat different than that found by Steyn (2003) in Eq. 4, based on observations. This deviation from the results of Steyn (2003) for the sea-breeze depth scaling was also found in the analysis of TVM model output in simulations using the Therry and Lacarrère (1983) turbulence closure scheme, and from (personal communication from A. Martilli 2004) model output from the FVM mesoscale model (Clappier et al. 1996; Martilli 2003). Martilli (2003) found by varying surface moisture content in the FVM model that Z_{sb}/z_s behaves similarly to Eq. 10. D.G. Steyn (personal communication 2005) confirms that simulations using two other mesoscale models (SAIMM and RAMS) result in the same sea-breeze depth scaling as TVM. In Porson (2005), this deviation is shown to be due to the presence of elevated stable layers imposing an internal length scale on the sea-breeze circulation (The systematic underestimation of the model relative to observations in Fig. 4 indicates indeed that the frequency N measured in the observations is larger than in the numerical experiments due to the presence of stable elevated layers).

This analysis of sea-breeze depth scaling combined with sea-breeze speed scaling allows us to define a scale for the volume flux VF_{sb} by the product of u_{sscale} and z_{sscale}:

$$u_{sscale}z_{sscale} = VF_{scale} = \frac{gH}{T\omega N}. \tag{12}$$

Figure 5 shows clearly that the volume flux VF_{sb} is well scaled by VF_{scale}:

$$VF_{sb} = 0.17\,VF_{scale}^{1.028}, \tag{13}$$

with a standard error of estimate on the exponent of 0.016. Note that VF_{scale} is not in disagreement with Steyn (2003) since VF_{scale} is also equal to the product of u_s and z_s from Steyn. As stated earlier, the non-scaled plot in Fig. 5 shows that the present results are not influenced by hidden correlation.

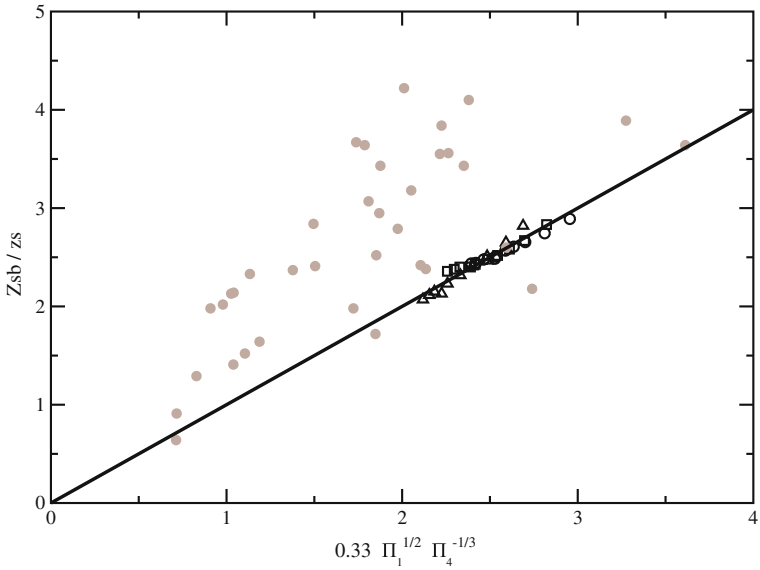

Fig. 4 TVM data for $[Z_{sb}/z_s]$ as a function of the regression in Eq. 10. The full black line is the one to one relationship. Ten groups of stability γ_i are represented for 1400 LST (circles), 1500 LST (squares) and 1600 LST (triangles). Observations of Vancouver (Steyn 2003) are also plotted in grey and filled circles

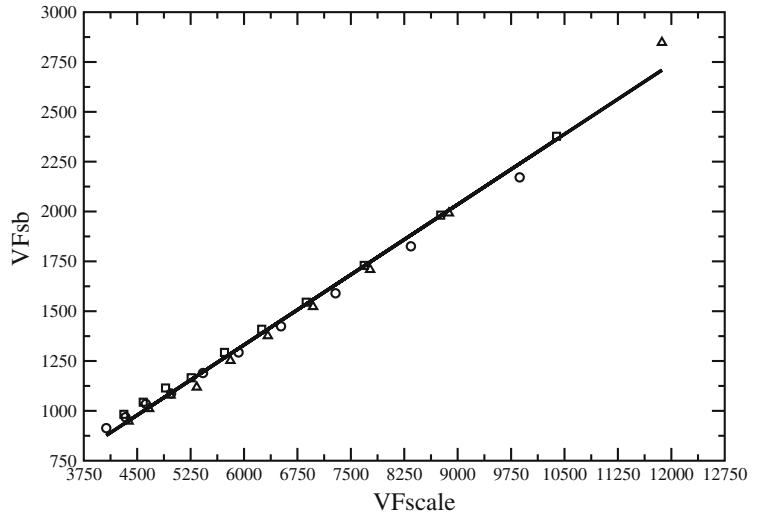

Fig. 5 TVM data for VF_{sb} as a function of VF_{scale}. Ten groups of stability γ_i are represented for 1400 LST (circles), 1500 LST (squares) and 1600 LST (triangles). The black line is a power law regression: $y = 0.17x^{1.03}$, with a standard error of estimate on the exponent of 0.02

4.2 The nature of the equilibrium

The volume flux scaling reflects an equilibrium in the sea-breeze circulation between the advection of stable air in the inflow layer of the sea-breeze circulation and the accumulated convergence of heat over land:

$$U_{\mathrm{sb}}\, Z_{\mathrm{sb}} = 0.17\, VF_{\mathrm{scale}}, \tag{14}$$

and

$$U_{\mathrm{sb}}\, Z_{\mathrm{sb}}\, N = 0.17\, \frac{gH}{T\omega}. \tag{15}$$

Indeed, the volume flux scale can be interpreted as reflecting an equilibrium for a fixed time in the afternoon. As noted earlier, the time-integrated surface heat flux is roughly constant in the afternoon period. We could not expect to obtain the same scaling laws if the period of analysis referred to the whole day and showed significant variations in the integrated surface heat flux — see Steyn (2003) and Wichink Kruit et al. (2004) for a comparison between one-day scaling analysis and maximum sea-breeze intensity analysis. The existence of an equilibrium in the sea-breeze cell was also reported by Finkele et al. (1995), who showed that the baroclinicity vector of the sea-breeze circulation in the sea-breeze cell (not in the front) is equal to zero, which under the Bjerknes circulation theorem suggests that the derivative of the sea-breeze circulation is zero. We can interpret this equilibrium in Eq. 15 thermodynamically by a consideration of the equation of conservation of thermal energy in stationary conditions under the Boussinesq approximation:

$$\underbrace{\frac{\partial\theta}{\partial t}}_{I} = \underbrace{-\overline{U}_j\frac{\partial\overline{\theta}}{\partial x_j}}_{II} + \underbrace{\nu_\theta\frac{\partial^2\overline{\theta}}{\partial x_j}}_{III} \underbrace{-\frac{1}{\overline{\rho}C_p}\frac{\partial\overline{Q_j^*}}{\partial x_j}}_{IV} \underbrace{-\frac{L_v E}{\overline{\rho}C_p}}_{V} \underbrace{-\frac{\partial(\overline{u_j'\theta'})}{\partial x_j}}_{VI}. \tag{16}$$

Term I represents heat storage, Term II represents advection, Term III represents molecular conduction of heat (with ν_θ being the thermal diffusivity), Term IV represents radiation divergence, Term V represents latent heat release (with L_v the latent heat associated with the phase change of E (mass of water vapour per unit volume per unit time being created by a phase change) and C_p the specific heat of moist air at constant pressure), and finally Term VI represents turbulent heat flux. Sea breezes are thus circulations in which the advection of stable air compensates for the creation of surface instability. Neglecting molecular conduction, condensation, radiative effects and vertical motions (sea-breeze circulations are hydrostatic, apart from processes in the vicinity of the front), Eq. 16 in stationary conditions is given by

$$\frac{\partial\theta}{\partial t} = 0 = -\overline{U}_1\frac{\partial\overline{\theta}}{\partial x_1} - \frac{\partial(\overline{u_3'\theta'})}{\partial x_3}, \tag{17}$$

with the indices 1 and 3 denoting horizontal and vertical directions, respectively. Equation 17 thus suggests a balance between the horizontal advection of horizontal temperature differences and the vertical derivative of the vertical heat flux.

We may thus interpret Eq. 17 for a sea-breeze circulation given the following considerations:

– Equation 17 must be integrated over the flow depth Z_{sb} and over the time period elapsed since sunrise t_{p}.

– In sea-breeze circulations, $\partial\theta/\partial x$ can be approximated by $\triangle T/x_s$ with x_s representing the horizontal length scale of the circulation. $\triangle T$ represents the temperature difference between land and sea air over the flow depth.
– Heating input arises primarily from the surface.

Vertical integration leads to:

$$\frac{1}{Z_{sb}}\int_0^{Z_{sb}} U_1\left(\frac{\triangle T}{x_s}\right)\mathrm{d}z = \frac{1}{Z_{sb}}\int_0^{Z_{sb}}\frac{\partial(\overline{w'\theta'})_s}{\partial z}\,\mathrm{d}z. \tag{18}$$

Since U_{sb} is defined as:

$$U_{sb} = \frac{1}{Z_{sb}}\int_0^{Z_{sb}} U_1\,\mathrm{d}z, \tag{19}$$

and since surface heat flux is independent of z, Eq. 18 yields:

$$\frac{\triangle T}{x_s}U_{sb} = \frac{(\overline{w'\theta'})_s}{Z_{sb}}. \tag{20}$$

Integration of Eq. 20 over time since sunrise gives:

$$\frac{U_{sb}Z_{sb}}{t_p}\int_0^{t_p}\frac{\triangle T}{x_s}\,\mathrm{d}t = \frac{1}{t_p}\int_0^{t_p}(\overline{w'\theta'})_s\,\mathrm{d}t = H, \tag{21}$$

with H the time-averaged surface heat flux. Multiplying Eq. 21 by $g/T\omega$ yields:

$$U_{sb}Z_{sb}\frac{1}{t_p}\int_0^{t_p}\frac{g}{T\omega}\frac{\triangle T}{x_s}\,\mathrm{d}t = \frac{gH}{T\omega} \tag{22}$$

and comparing Eq. 22 with Eq. 15 leads to:

$$N\omega \approx \frac{1}{t}\int_0^{t_p}\frac{g}{T}\frac{\triangle T}{x_s}\,\mathrm{d}t. \tag{23}$$

As mentioned earlier, Eq. 23 can also be interpreted in terms of the Bjerknes circulation theorem, which requires that the total derivative of the circulation (line integral) equals the baroclinicity vector. In the present case, with the circulation confined to the vertical $(x_1 - x_3)$ plane, it is the x_2-component of the baroclinicity vector that is dependent on α, the specific volume:

$$\frac{\mathrm{d}C_{SB}}{\mathrm{d}t} = \frac{\partial\alpha}{\partial x_1}\frac{\partial p}{\partial x_3} - \frac{\partial\alpha}{\partial x_3}\frac{\partial p}{\partial x_1}. \tag{24}$$

Equation 24 suggests that variations in density are linked to variations in pressure, and that the horizontal gradients of pressure and density balance the vertical gradients of these two variables. This balance between the horizontal and the vertical gradients is similar to the balance of the gradients of potential temperature in Eq. 23.

5 Conclusions

The present study has shown that the TVM model is capable of capturing the scaling of sea-breeze speed from the most recent findings. The flexibility of the model has been exploited to explore sea-breeze depth and volume flux scaling.

While sea-breeze speed scale depends only on surface heating, sea-breeze depth scale depends also on stability. A sea-breeze depth scale was derived from simplified convective conditions.

Together, the speed and depth scales provide a volume flux scale that reflects an equilibrium at a fixed time in the afternoon between firstly, convergence of heat over land accumulated since sunrise, and secondly, advection of stable air from the sea surface. This equilibrium confirms similar previous findings based on the circulation theorem and is expressed here in terms of the governing variables of the sea-breeze circulation.

Acknowledgements This study was supported by Fonds pour la Formation à la Recherche dans l'Industrie et dans l'Agriculture, Belgium and the Natural Science and Engineering Research Council of Canada, the Belgian National Fund for Research and the French Community of Belgium. Special thanks are due to Alberto Martilli and Terry Clark for help with modelling questions.

References

Arritt R (1987) The effect of water surface temperature on lake breezes and thermal internal boundary layers. Boundary-Layer Meteorol 40:101–125

Arritt R (1989) Numerical modelling on the offshore extent of sea breezes. Quart J Roy Meteorol Soc 115:547–570

Bougeault P, Lacarrère P (1989) Parameterization of orography-induced turbulence in a Mesobeta-Scale model. Mon Wea Rev 117:1872–1890

Clappier A, Perrochet P, Martilli A, Muller F, Krueger BC (1996) A new non-hydrostatic mesoscale model using a control volume finite element (CVFE) discretisation technique. In: PM Borrell et al. (eds) Proceedings of EUROTRAC symposium 96. Computational Mechanics Publications, Southampton, U.K., 527–531

Deardoff J (1978) Efficient prediction of ground surface temperature and moisture, with inclusion of a layer of vegetation. J Geophys Res 83:1198–1903

Finkele K, Hacker JM, Kraus H, Byronscott R (1995) A complete sea-breeze circulation cell-derived from aircraft observations. Boundary-Layer Meteorol 73(3):299–317

Martilli A (2003) A two-dimensional numerical study of the impact of a city on atmospheric circulation and pollutant dispersion in a coastal environment. Boundary-Layer Meteorol 108:91–119

Pielke RA, Segal M (1986) Mesoscale circulations forced by differential terrain heating. In: PS Ray (ed) Mesoscale meteorology and forecasting. Amer Meteorol Soc, Boston, 793 pp, chapter 22, pp. 516–548

Porson A (2005) Sea breeze Scaling in idealized conditions: the influence of topography and large-Scale winds, Ph.D Dissertation, Université catholique de Louvain, Louvain-la-Neuve, Belgium, 259 pp

Raymond WH, Garder A (1988) A spatial filter for use in finite area calculations. Mon Wea Rev 116:209–222

Schayes G, Thunis P, Bornstein R (1996) Topographic vorticity-mode mesoscale-beta (TVM) model. Part I: formulation. J Appl Meteorol 35:1818–1823

Simpson JE (1969) A comparison between laboratory and atmospheric density currents. Quart J Roy Meteorol Soc 95:758–765

Steyn DG (1998) Scaling the vertical structure of sea breezes. Boundary-Layer Meteorol 86:505–524

Steyn DG (2003) Scaling the vertical structure of sea breezes revisited. Boundary-Layer Meteorol 107:177–188

Stull RB (1988) An introduction to boundary layer meteorology. Kluwer Academic Publishers, Dordrecht, The Netherlands, 666 pp

Therry G, Lacarrère P (1983) Improving the Eddy kinetic energy model for planetary boundary layer description. Boundary-Layer Meteorol 25:63–88
Thunis P, Clappier A (2000) Formulation and evaluation of a Non-Hydrostatic meoscale vorticity model (TVM). Mon Wea Rev 128:3236–3250
Tijm ABC, van Delden AJ, Holtslag AAM (1999a) The inland penetration of sea breezes. Contr Atmos Phys 72(4):317–328
Tijm ABC, Holtslag AAM, van Delden AJ (1999b) Observations and modeling of the sea breeze with the return current. Mon Wea Rev 127:625–640
Walsh JE (1974) Sea breeze theory and applications. J Atmos Sci 31:2012–2026
Wichink Kruit RJ, Holtslag AAM, Tijm ABC (2004) Scaling of the sea-breeze strength with observations in the Netherlands. Boundary-Layer Meteorol 112:369–380